8-10-2018

Spatial distribution of organic functional groups supported on mesoporous silica nanoparticles (2): a study by 1H triple-quantum fast-MAS solid-state NMR

Takeshi Kobayashi
Ames Laboratory, takeshi@ameslab.gov

Dilini Singappuli-Arachchige
Iowa State University and Ames Laboratory, dilini@iastate.edu

Igor I. Slowing
Iowa State University and Ames Laboratory, islowing@iastate.edu

Marek Pruski
Iowa State University and Ames Laboratory, mpruski@iastate.edu

Spatial distribution of organic functional groups supported on mesoporous silica nanoparticles (2): a study by 1H triple-quantum fast-MAS solid-state NMR

Abstract

The distribution of organic functional groups attached to the surface of mesoporous silica nanoparticles (MSNs) via co-condensation was scrutinized using 1D and 2D 1H solid-state NMR, including the triple-quantum/single-quantum (TQ/SQ) homonuclear correlation technique. The excellent sensitivity of 1H NMR and high resolution provided by fast magic angle spinning (MAS) allowed us to study surfaces with very low concentrations of aminopropyl functional groups. The sequential process, in which the injection of tetraethyl orthosilicate (TEOS) into the aqueous mother liquor was followed by dropwise addition of the organosilane precursor, resulted in deployment of organic groups on the surface, which were highly clustered even in a sample with a very low loading of ~0.1 mmol g−1. The underlying mechanism responsible for clustering could involve fast aggregation of the aminopropyltrimethoxysilane (APTMS) precursor within the liquid phase, and/or co-condensation of the silica-bound molecules. Understanding the deposition process and the resulting topology of surface functionalities with atomic-scale resolution, can help to develop novel approaches to the synthesis of complex inorganic–organic hybrid materials.

Disciplines

Chemistry | Nanoscience and Nanotechnology | Organic Chemistry | Physical Chemistry

Comments

This is a manuscript of an article published as Kobayashi, Takeshi, Dilini Singappuli-Arachchige, Igor I. Slowing, and Marek Pruski. "Spatial distribution of organic functional groups supported on mesoporous silica nanoparticles (2): a study by 1 H triple-quantum fast-MAS solid-state NMR." *Physical Chemistry Chemical Physics* 20, no. 34 (2018): 22203. DOI: 10.1039/C8CP04425B. Posted with permission.

View Article Online
DOI: 10.1039/C8CP04425B

Spatial distribution of organic functional groups supported on mesoporous silica nanoparticles (2): a study by ^{1}H triple-quantum fast-MAS solid-state NMR

Takeshi Kobayashi,[†] Dilini Singappuli-Arachchige,[†,‡] Igor I. Slowing,[†,‡,*] Marek Pruski[†,‡,*]

[†]U.S. DOE Ames Laboratory, Iowa State University, Ames, Iowa 50011, United States

[‡]Department of Chemistry, Iowa State University, Ames, Iowa 50011, United States

*Corresponding author.
M. Pruski: Ames Laboratory, Iowa State University, 230 Spedding Hall, Ames, IA 50011-3020, USA. Phone: +1 515 294 2017 Fax: +1 515 294 4709. E-mail address: mpruski@iastate.edu.

View Article Online
DOI: 10.1039/C8CP04425B

Abstract

The distribution of organic functional groups attached to the surface of mesoporous silica nanoparticles (MSNs) via co-condensation was scrutinized using 1D and 2D ^{1}H solid-state NMR, including triple-quantum/single-quantum (TQ/SQ) homonuclear correlation technique. The excellent sensitivity of ^{1}H NMR and high resolution provided by fast magic angle spinning (MAS) allowed us to study surfaces with very low concentrations of aminopropyl functional groups. The sequential process, in which the injection of tetraethyl orthosilicate (TEOS) into the aqueous mother liquor was followed by dropwise addition of the organosilane precursor, resulted in deployment of aggregated organic groups on the surface, which were dominant even in a sample with a very low loading of ~0.1 mmol/g. The underlying mechanism responsible for clustering could involve fast aggregation of aminopropyltrimethoxysilane (APTMS) precursor within the liquid phase, and/or co-condensation of the silica-bound molecules. Understanding the deposition process and the resulting topology of surface functionalities with atomic-scale resolution, can help to develop novel approaches to the synthesis of complex inorganic-organic hybrid materials.

View Article Online
DOI: 10.1039/C8CP04425B

1. INTRODUCTION

Since the discovery of surfactant-templated synthesis of mesoporous silica materials,[1] many research efforts have been directed toward tuning the shape of particles, pore topology and surface area.[2-6] Further tailoring of these materials, herein referred to as mesoporous silica nanoparticles (MSNs), for specific applications can be achieved by functionalization with organic moieties.[7-9] Endeavors have focused on not only refining the chemical properties of these functional units in the resulting inorganic–organic hybrids but also on regulating their spatial arrangement.[8, 10-13] Assessing the uniformity of surface functionalization within the pores with atomic-scale precision is of great importance, but is also very challenging. Previously, such studies relied on the use of relatively bulky probe molecules, falling short of the required sub-nm resolution.[14-18]

Recently, we investigated the spatial distribution of functional groups covalently attached to MSNs using solid-state (SS)NMR spectroscopy, notably using the dynamic nuclear polarization (DNP)-enhanced two-dimensional (2D) ^{29}Si–^{29}Si double-quantum/single-quantum (DQ/SQ)[19] and 2D ^{13}C–^{13}C SQ/SQ correlation experiments at natural abundance.[20] The former study revealed that post-synthesis grafting leads to a more homogeneous dispersion of organic functionalities than the co-condensation method. During the grafting process under anhydrous condition, the organosilane precursors do not self-condense and are unlikely to bond to the silica surface in close proximity. The latter study investigated the spatial distribution of *different* types of functional groups on the surface of a bifunctional system prepared using the co-condensation method; its results suggested that i) the functionalities formed clusters and were unevenly distributed on the silica surface, and ii) within the clusters the functional groups were well mixed with each other. In these studies, the samples contained relatively high loading of functional

View Article Online
DOI: 10.1039/C8CP04425B

groups, ≥ ~2 mmol/g. Upon further dilution of species, however, it remains a challenge to observe homonuclear correlations between insensitive nuclei even with the tremendous sensitivity enhancement offered by DNP.

Through-space ^{1}H–X heteronuclear correlation (HETCOR) spectroscopy can provide information about the structure, conformation, and dynamics of complex molecular systems.[21-23] However, the low efficiency of long-range polarization and dipolar truncation effects favor recoupling of short-range dipolar interactions in most materials, yielding primarily intramolecular correlations.[24] Owing to the excellent sensitivity and the ubiquity of ^{1}H, ^{1}H–^{1}H SQ/SQ spin-diffusion and DQ/SQ MAS experiments have been commonly used for gaining structural insights into a wide range of materials including heterogeneous catalysts,[25] self-assembled supra molecules,[22] and inorganic-organic hybrid materials.[26] Thus, our present efforts focused on the fast MAS-based ^{1}H–^{1}H correlation methods. In the SQ/SQ spin-diffusion method, diagonal peaks result not only from the diffusive spin exchange between equivalent protons (correlations **a** and **b** in Figure 1) but also from unwelcome non-exchanged magnetization (correlation **c** in Figure 1). Meanwhile, the cross peaks represent an inter-spin exchange of magnetization between non-equivalent protons (interactions **d** and **e** in Figure 1). The DQ/SQ experiment filters out the signals from non-exchanged magnetization (correlation **c** in Figure 1) and provides much 'cleaner' spectra than the SQ/SQ scheme. However, neither SQ/SQ nor DQ/SQ can discriminate between intra- and intermolecular correlation signals when the single molecule has two or more equivalent protons, as in methylene and methyl groups. Thus, higher-order of multiple-quantum filtering is required to probe the spatial distribution of similar functional groups through ^{1}H–^{1}H correlation experiments.[27, 28] For example, the triple quantum (TQ) correlation[27-31] from two equivalent methylene groups, depicted as correlation **f** in Figure 1,

View Article Online
DOI: 10.1039/C8CP04425B

will exclusively represent the intermolecular interactions, provided that ^{1}H resonances from different CH_2 groups in a given molecule can be sufficiently resolved by fast MAS.

In the present study, we used the ^{1}H TQ/SQ correlation technique to determine the spatial distribution of organic (aminopropyl) moieties deposited on MSNs' surfaces by co-condensation with loadings as low as 0.14 mmol/g.

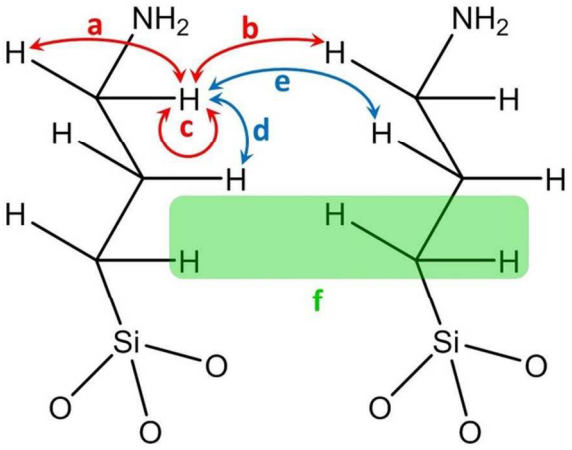

Figure 1. Schematic illustration of homonuclear correlation experiments.

2. EXPERIMENTAL SECTION

2.1. Sample Preparations.

Aminopropyl-functionalized MSNs (AP-MSN) were prepared as follows. In a round-bottom flask, cetyltrimethylammonium bromide (CTAB, 1.0 g, 2.74 mmol) was dissolved in deionized water (480 ml), followed by addition of a 2 M aqueous solution of NaOH (3.5 mL, 7.0 mmol). The solution was stirred for 1 h at 80 °C. Tetraethyl orthosilicate (TEOS, 5.0 mL, 22.6 mmol) was added dropwise over 6 min, followed by dropwise addition of aminopropyltrimethoxysilane (APTMS, 1.0 mL, 5.73 mmol) over 1 min to the CTAB solution. Magnetic stirring was continued for another 2 h at 80 °C. The solution was filtered, washed with

View Article Online
DOI: 10.1039/C8CP04425B

excess water and methanol, and vacuum-dried overnight. The CTAB template was removed by refluxing 1.0 g of the dry solid with a mixture of methanol (100 mL) and concentrated HCl (0.8 mL, 9.7 mmol) at 60 °C for 6 h. The surfactant-removed sample was again filtered, washed with excess methanol and vacuum-dried overnight. MSN samples with lower loading of functionalities were also prepared by decreasing the amount of APTMS precursor to 0.18 mL (1.03 mmol) or 0.090 mL (0.52 mmol) in the original procedure. To minimize the ^{1}H background, the surface silanols were deuterated by suspending the AP-MSN samples in $^{2}H_2O$ overnight, after which the supernatant was decanted. The ^{1}H–^{2}H exchange also included the terminal amine moiety of AP. The resultant $^{2}H_2O$-exchanged samples were vacuum-dried at room temperature and quickly transferred to the magic-angle spinning (MAS) zirconia rotors. The AP-MSN samples are denoted as AP-x, where "x" indicates loading of the aminopropyl groups (AP).

2.2. Solid-state NMR.

To confirm the surface functionalization and determine the concentration of AP groups in the studied samples, we carried out conventional ^{29}Si direct polarization (DP)MAS and DNP-enhanced $^{13}C\{^{1}H\}$ cross-polarization (CP)MAS experiments described in the Electronic supplementary information (ESI, see Figures S1 and S2).

The ^{1}H SSNMR experiments were performed on a Varian NMR spectrometer, equipped with a 1.6-mm triple-resonance MAS probe and operated at 14.1 T. Several one- and two-dimensional (1D and 2D) experiments were carried out, including 1D ^{1}H MAS, ^{1}H transverse relaxation time (T_2') measurement, and 2D ^{1}H TQ/SQ MAS NMR. All experiments were performed under fast MAS at a rate of 36 kHz. The T_2' relaxation times of ^{1}H nuclei were measured using a spin–echo sequence without ^{1}H–^{1}H radio-frequency (RF) homonuclear decoupling. The TQ/SQ correlation experiments used a BABA-16 sequence for homonuclear

View Article Online
DOI: 10.1039/C8CP04425B

recoupling,[32] where the recoupling pulses were flanked by a $\pi/2$ pulse at the beginning of the excitation period and at the end of the reconversion period, thereby exciting triple-quantum (and higher odd order) coherence (see Figure 2).[30] The sequence was first tested on L-alanine and verified by comparing the spectrum with that reported in an earlier study[27] (see Figure S3 in ESI). ^{1}H chemical shifts were referenced with respect to tetramethylsilane (TMS) at 0 ppm. In the TQ dimension of the TQ/SQ MAS spectra, the observed ^{1}H shifts were given as the sums of the SQ shifts of the three nuclei involved.

The experimental parameters are given in figure captions, where $\nu_R = (\tau_R)^{-1}$ is the MAS rate, $\nu_{RF}(X)$ is the magnitude of the RF magnetic field applied to X spins, $\tau_{exc/rec}$ is the SQ-TQ excitation time/TQ-SQ reconversion time, τ_z is the z-filter delay, Δt_1 is the increment of t_1 during 2D acquisition, τ_{RD} is the recycle delay, NS is the number of scans per row, and AT is the total acquisition time.

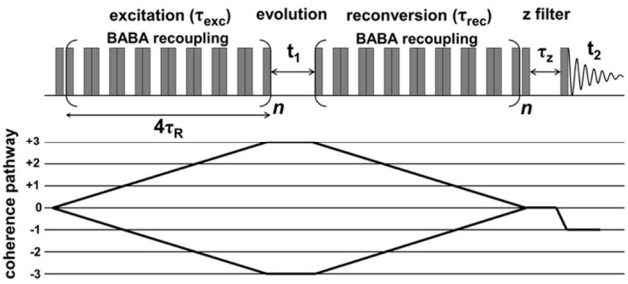

Figure 2. Pulse sequence used for TQ MAS experiment and the coherence transfer pathway. Shaded rectangular bars represent hard $\pi/2$ pulses.

3. RESULTS AND DISCUSSION

We first estimated the amounts of organic groups introduced into each sample as follows. We carried out a 1D ^{29}Si direct polarization (DP)MAS experiment (see Figure S2 in ESI) for the sample with highest loading, and determined the amount of functionalities through the

View Article Online
DOI: 10.1039/C8CP04425B

concentration of T^n sites to be 1.24 mmol/g; this sample was referred to as AP-1.2. Although this experiment can provide quantitative concentration of functionalities in the highly loaded sample (here with an accuracy of 10%[9, 12]), it is difficult to determine the concentration of T^n sites in the samples with lower loading by this method, because of low signal intensity. Therefore, we used the DNP-enhanced $^{13}C\{^1H\}$ CPMAS spectra (Figure S2 in ESI) to accurately estimate the *relative* loading of functionalities in our samples, by safely assuming the same CP dynamics among those samples under the DNP condition. By comparing the ^{13}C signal intensities from the sparsely populated surfaces to that of AP-1.2, the concentrations of functionalities were estimated to be 0.39 and 0.14 mmol/g (referred to as AP-0.4 and AP-0.1, respectively). Taking into account that the surface areas of AP-1.2, AP-0.4, and AP-0.1 were measured at 890, 1072, and 1020 m^2/g, the amounts of AP molecules per 1 nm^2 in these samples are ~ 0.8, 0.2 and 0.08, respectively. On the uniformly functionalized surfaces, these coverages would correspond to *average* AP-AP distances of approximately 1.1 nm (AP-1.2), 2.2 nm (AP-0.4) and 3.6 nm (AP-0.1). The DNP-enhanced $^{13}C\{^1H\}$ CPMAS spectra also confirmed a complete removal of CTAB.

1D ^1H DPMAS spectra of AP-1.2 and AP-0.4 showed three relatively sharp signals at 0.64, 1.65, and 2.87 ppm, assigned to the protons in the three methylene groups of AP (Figure 3).[33] As a cross-check, we verified that the relative integrated intensity of these signals is consistent with the loadings of functionalities estimated by the ^{29}Si DPMAS and DNP-enhanced $^{13}C\{^1H\}$ CPMAS experiments. A strong signal centered at ~4.5 ppm is attributed to weakly bound, mobile water.[34, 35] The ^1H signal of the terminal NH_2 did not appear because this moiety has exchanged with ^2H. In the ^1H DPMAS spectrum of AP-0.1, however, the methylene signals appeared in association with sub-signals separated from H1, H2 and H3 by ~0.3 ppm (~180 Hz), referred to as H1′, H2′, and H3′, respectively. Those sub-signals suggest the existence of two

View Article Online
DOI: 10.1039/C8CP04425B

populations of aminopropyl groups residing on the silica surface in different environments, which do not exchange on the time scale of $(180\ \text{Hz})^{-1} \approx 4.8$ ms. For reasons to be discussed in paragraphs below, we denoted the aminopropyl groups involving H1~H3 and H1′~H3′ as AP_{agg} and AP_{iso}, respectively. A small signal at ~3.5 ppm was attributed to protons of methoxy groups which remained after the ^2H_2O treatment. The signal at 0.1 ppm was not assigned to any known species.

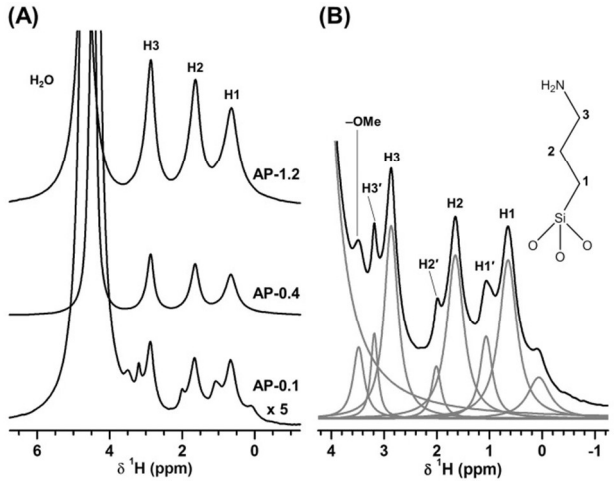

Figure 3. ^{1}H DPMAS spectra of AP-MSNs (A) and the deconvolution of ^{1}H DPMAS spectrum of AP-0.1 (B). The spectra were obtained using ν_R = 36 kHz; $\nu_{RF}(^1H)$ = 100 kHz; τ_{RD} = 1.5 s (AP-1.2 and AP-0.4) and 2.0 s (AP-0.1); NS = 16.

The T_2' relaxation times of ^{1}H nuclei measured by the spin–echo sequence are listed in Table 1. We first note that given the fast MAS rate used in our measurements, the observed values are consistent with limited librational rotations of surface-immobilized molecules.[36] The T_2' times of H2 and H3 were only slightly longer than that of H1 in directly surface-bound methylene, suggesting the overall restricted mobility of AP_{agg}. Furthermore, the T_2' values for the corresponding methylene protons H1, H2, and H3 were similar among the samples, indicating that the mobility of AP_{agg} molecules is independent of the loading in the range used in this study.

View Article Online
DOI: 10.1039/C8CP04425B

In contrast, the T_2' values of H2′ and H3′ were significantly larger than that of H1′, and also exceeded those of H2 and H3. These results indicate that the AP_{iso}, which was detectable only in the AP-0.1 sample, has increased mobility toward the amine end, stemming from reduced AP–AP and/or AP–surface interactions.

Table 1. Transverse Relaxation Time, T_2' (ms).

Samples	H1	H1′	H2	H2′	H3	H3′
AP-1.2	1.5±0.1		1.7±0.1		2.1±0.1	
AP-0.4	1.5±0.1		1.6±0.1		2.0±0.1	
AP-0.1	1.4±0.1	1.6±0.2	1.5±0.1	2.9±0.1	1.9±0.2	3.3±0.2

The differences between aggregated and isolated molecules, and their interactions with surface, can also be manifested through shifts in NMR resonance frequency.[37-39] For example, we have recently demonstrated that the local polarity at the surface of functionalized MSNs materials depends on the density of functional groups.[40] In the present study, the 0.3 ppm difference in the observed shifts between H and H′ hydrogens is most likely attributable to the changes of electron density distribution between clustered and isolated groups, although more precise interpretation of this shift would require further study. Taken together, the relaxation and chemical shift data point to the existence of two populations of AP species, identified as agglomerated and isolated aminopropyl groups, AP_{agg} and AP_{iso}, respectively. The vast preponderance of AP_{agg} in AP-1.2 and AP-0.4, and the emergence of AP_{iso} in AP-0.1, further corroborate the above identification.

The spatial distribution of organic functionalities was directly confirmed using 2D ^{1}H TQ/SQ correlation experiments. The AP-1.2 and AP-0.4 samples showed practically identical correlation spectra (Figure 4A and B), where all possible TQ correlation signals appeared after

View Article Online
DOI: 10.1039/C8CP04425B

the excitation/reconversion time $\tau_{exc/rec} = 4\tau_R$ (111.1 μs). The correlation signals involving physisorbed water were not identified (the missing cross peaks would be expected at δ_{SQ}/δ_{TQ} = 0.64/5.78, 0.64/9.64, and 1.65/7.80) within the presented spectral region due to motional averaging of the dipolar coupling. The off-diagonal cross peaks arising from distant methylene groups, i.e. H1–H1–H3 and H1–H3–H3, were weaker than those from nearby methylene groups. As expected, the correlation signals assigned to H1–H2–H3 showed the lowest intensities. These cross peaks potentially arise from both intra- and intermolecular correlations. In contrast to cross peaks, the diagonal peaks *can only originate from intermolecular correlations*, because more than one AP must be present to create a TQ correlation signal of a spin triad among equivalent protons.

It is important to remark here that the SQ-TQ excitation and TQ-SQ reconversion processes rely on ^{1}H-^{1}H dipolar interactions, which exhibit an inverse cubed dependence on internuclear distance; thus, the TQ coherences can be only induced between ^{1}H nuclei remaining in close proximity to each other. For example, numerical simulations of the BABA recoupling sequence by SIMPSON[41] showed that the correlation signal for ^{1}H spins situated at the corners of an equilateral triangle with a side of 0.18 nm (as in methylene group) is about 30 times more intense than for an isosceles triangle with the sides of 0.18, 0.5 and 0.5 nm. Given the average AP-AP distances calculated above for AP-1.2 (1.05 nm), AP-0.4 (1.9 nm) and AP-0.1 (3.2 nm), no intermolecular coherences would be detectable in any of these samples if the surfaces were indeed uniformly functionalized. Thus, the appearance of diagonal signals unambiguously indicates the close proximities of functionalities (<0.5 nm), which further substantiates the assignment of H1, H2 and H3 resonances to the clustered aminopropyl groups, i.e. AP_{agg}. Figure 4C shows the build-up of H1–H1–H1 with the increase of recoupling time. Since the intensities

View Article Online
DOI: 10.1039/C8CP04425B

of all correlation peaks monotonically decreased with the increase of recoupling time, those spectra are presented relative to one of the H1–H1–H2 cross peaks at δ_{SQ}/δ_{TQ} = 0.64/2.93. Surprisingly and very importantly, the relative intensities of the H1–H1–H1 correlation signals and their time evolutions observed for AP-0.4 were very similar to those of AP-1.2. This result indicates that the spatial distributions of APs on the surface of AP-1.2 and AP-0.4 samples are independent of coverage, and are dominated by AP_{agg}. The fact that the H3-H3-H3 cross-peaks in AP-1.2 and AP-0.4 are more intense than H1-H1-H1, suggests that the terminal sections of AP molecules are in closer proximity than the silica-bound methylenes. Likely, hydrogen bonds between the amines attract the terminal moieties to each other and restrict their mobilities, while the lack of hydrogen bonds in the AP_{iso} results in the increased T_2' values near the amine end.

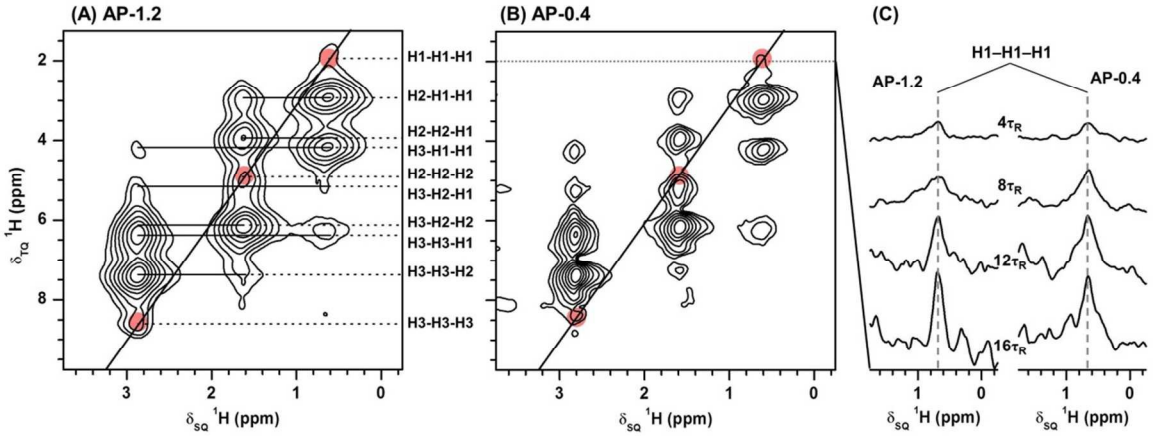

Figure 4. 2D ^{1}H TQ/SQ MAS correlation of AP-1.2 (A) and AP-0.4 (B), and slices of 2D TQMAS spectra at δ_{TQ} = 2.0 ppm (C). The TQMAS spectra were obtained using ν_R = 36 kHz, $\nu_{RF}(^1H)$ = 100 kHz, $\tau_{exc/rec} = 4\tau_R$ (111.1 μs), τ_z = 1 ms, τ_{RD} = 1.5 s, 256 rows with Δt_1 = 27.778 μs, NS = 24, and AT = 5.1 h. The sliced spectra (C) were normalized to the loading of functionalities contained in the sample rotors. Note that in the TQ dimension, the observed ^{1}H shift is the sum of the SQ shifts of the nuclei involved. Red circles represent the positions of the diagonal H1-H1-H, H2-H2-H2 and H3-H3-H3 peaks.

View Article Online
DOI: 10.1039/C8CP04425B

In the AP-0.1 sample, the H protons of AP_{agg} showed a similar set of correlation signals to those observed in AP-1.2 and AP-0.4. On the other hand, the 2D ^{1}H TQ/SQ experiment did not show any detectable correlation signals involving H′ protons of AP_{iso}, even after several days of data accumulation with increased recoupling time. We thus collected 1D TQ-filtered ^{1}H NMR spectra for the AP-0.1 (Figure 5B). With $\tau_{exc/rec} = 4\tau_R$ (111.1 μs), the signal of H2′ was barely detectable. When the recoupling time was increased to $\tau_{exc/rec} = 8\tau_R$ (222.2 μs), the spectrum showed an increase of the H2′ signal and the appearance of H1′, despite the severe decrease of H signal intensities. Unfortunately, the 1D TQ-filtered experiment could not discriminate between intra- and intermolecular interactions. However, the low efficiency and slow build-up of TQ/SQ transfers for H′ sites strongly suggest the lack of intermolecular interactions between AP_{iso} functionalities.

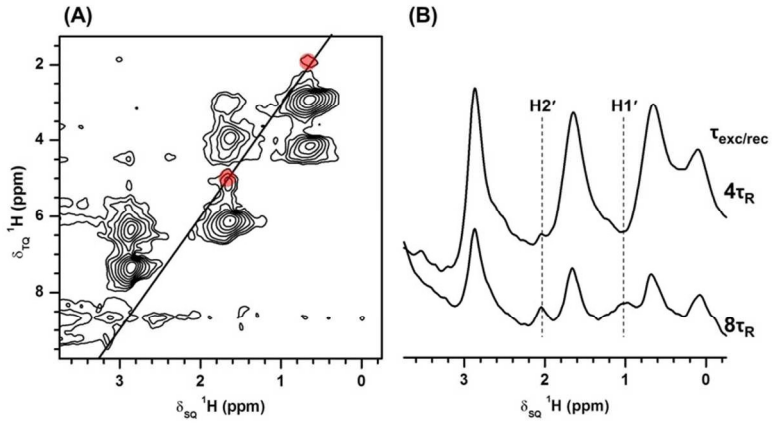

Figure 5. 2D ^{1}H TQ/SQ MAS and 1D TQ-filtered ^{1}H MAS spectra of AP-0.1. The spectra were obtained using ν_R = 36 kHz, $\nu_{RF}(^1H)$ = 100 kHz, τ_z = 1 ms, τ_{RD} = 2.0 s. The 2D ^{1}H TQ/SQ spectrum (A) was taken with $\tau_{exc/rec} = 4\tau_R$ (111.1 μs), 256 rows with Δt_1 = 27.778 μs, NS = 96, and AT = 27.3 h. The 1D TQ-filtered ^{1}H spectra (B) were collected using NS = 768.

The SSNMR results demonstrate that AP groups introduced by sequential co-condensation of TEOS and APTMS are predominantly clustered. Whether this clustering occurs via formation of $(AP\text{-}Si\text{-}O)_n$ oligomers prior to attachment to the growing silica polymer (model

View Article Online
DOI: 10.1039/C8CP04425B

I in Fig.6), through nucleation and growth on the polymer surface (model II in Fig.6), or through a ripening mechanism involving surface migration under the basic reaction conditions (model III in Fig.6), should depend on the relative rates of hydrolysis and condensation and the thermodynamic stability of the hydrophobic organic groups at the polymer/template/water interface. Multiple mechanisms can be possibly involved in the formation of clustered functionalized sites. Future elucidation of the clustering mechanism will provide additional insights to control the distribution of the organic groups on the surface and enable the development of increasingly complex materials for advanced applications.

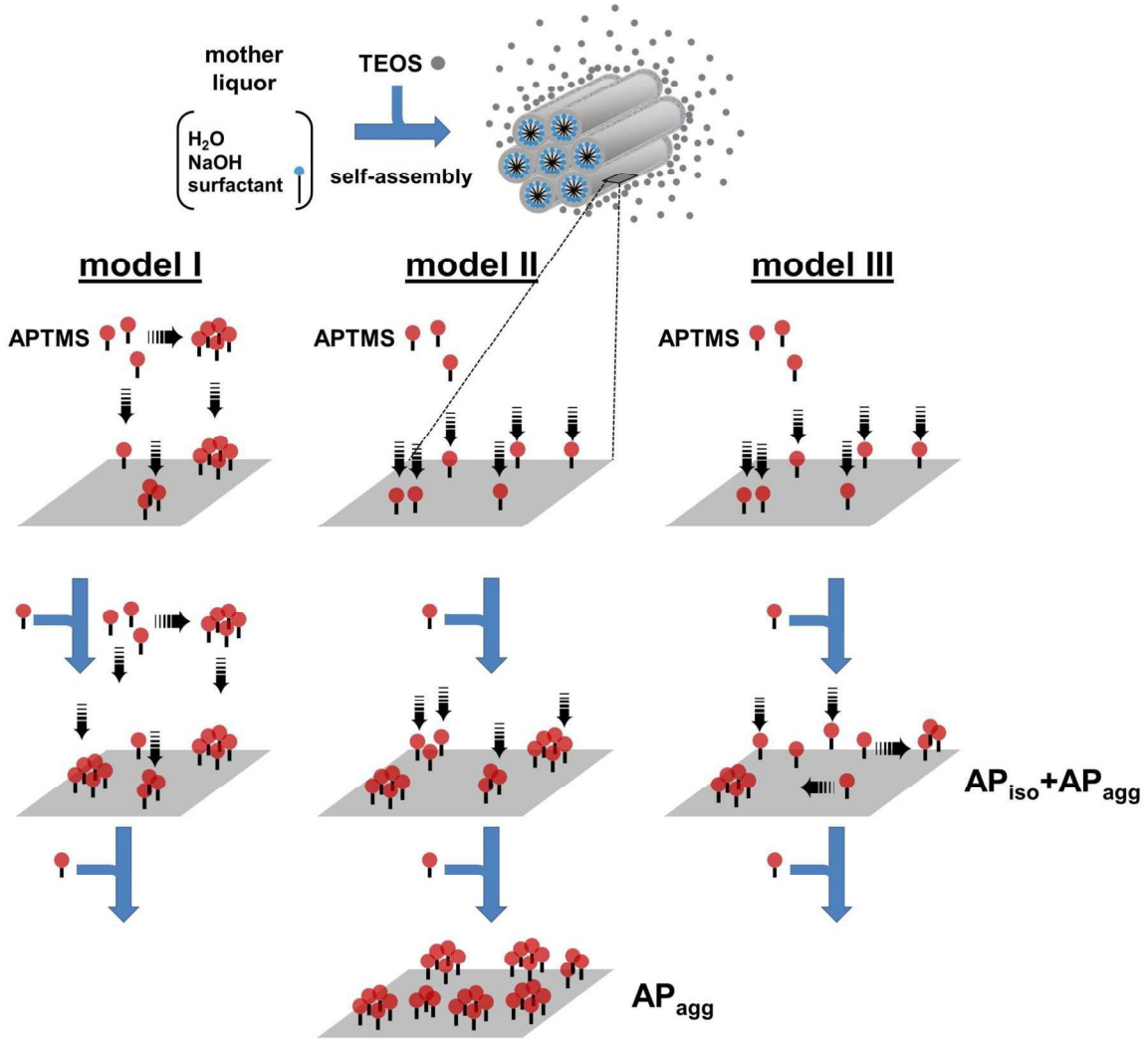

View Article Online
DOI: 10.1039/C8CP04425B

Figure 6. Suggested mechanism of the synthesis of AP-MSNs via co-condensation method using a sequential addition of TEOS followed by APTMS.

4. CONCLUSION

We used 1D and 2D ^{1}H SSNMR experiments to scrutinize the distribution of aminopropyl groups attached to the surfaces of MCM-41 type mesoporous silica materials synthesized by co-condensation. The TQ/SQ MAS correlation spectra revealed that the vast majority of the AP organic functional groups is agglomerated; even in the sample with a very low loading of 0.1 mmol/g only a small fraction remains isolated. The ability to monitor the spatial distribution of surface species will help study the underlying mechanisms of functionalization and achieve better synthetic control.

ACKNOWLEDGEMENTS

This research is supported by the U.S. Department of Energy, Office of Basic Energy Sciences, Division of Chemical Sciences, Geosciences, and Biosciences through the Ames Laboratory. The Ames Laboratory is operated for the U.S. Department of Energy by Iowa State University under Contract No. DE-AC02-07CH11358.

View Article Online
DOI: 10.1039/C8CP04425B

REFERENCES

1 C. T. Kresge, M. E. Leonowicz, W. J. Roth, J. C. Vartuli and J. S. Beck, *Nature*, 1992, **359**, 710-712.
2 J. S. Beck, J. C. Vartuli, W. J. Roth, M. E. Leonowicz, C. T. Kresge, K. D. Schmitt, C. T. W. Chu, D. H. Olson, E. W. Sheppard, S. B. McCullen, J. B. Higgins and J. L. Schlenker, *J. Am. Chem. Soc.*, 1992, **114**, 10834-10843.
3 S. A. Bagshaw, E. Prouzet and T. J. Pinnavaia, *Science*, 1995, **269**, 1242-1244.
4 D. Y. Zhao, J. L. Feng, Q. S. Huo, N. Melosh, G. H. Fredrickson, B. F. Chmelka and G. D. Stucky, *Science*, 1998, **279**, 548-552.
5 G. J. A. A. Soler-Illia and O. Azzaroni, *Chem. Soc. Rev.*, 2011, **40**, 1107-1150.
6 C. G. Goltner and M. Antonietti, *Adv. Mater.*, 1997, **9**, 431-436.
7 A. Stein, B. J. Melde and R. C. Schroden, *Adv. Mater.*, 2000, **12**, 1403-1419.
8 F. de Clippel, M. Dusselier, S. Van de Vyver, L. Peng, P. A. Jacobs and B. F. Sels, *Green Chem.*, 2013, **15**, 1398-1430.
9 S. Huh, J. W. Wiench, J. C. Yoo, M. Pruski and V. S. Y. Lin, *Chem. Mater.*, 2003, **15**, 4247-4256.
10 J. Kecht, A. Schlossbauer and T. Bein, *Chem. Mater.*, 2008, **20**, 7207-7214.
11 J. D. Webb, T. Seki, J. F. Goldston, M. Pruski and C. M. Crudden, *Microporous Mesoporous Mater.*, 2015, **203**, 123-131.
12 K. Hara, S. Akahane, J. W. Wiench, B. R. Burgin, N. Ishito, V. S. Y. Lin, A. Fukuoka and M. Pruski, *J. Phys. Chem. C*, 2012, **116**, 7083-7090.
13 F. de Juan and E. Ruiz-Hitzky, *Adv. Mater.*, 2000, **12**, 430-432.
14 J. C. Hicks, R. Dabestani, A. C. Buchanan, III and C. W. Jones, *Chem. Mater.*, 2006, **18**, 5022-5032.
15 R. Mouawia, A. Mehdi, C. Reye and R. Corriu, *New J. Chem.*, 2006, **30**, 1077-1082.
16 M. Sohmiya, Y. Sugahara and M. Ogawa, *J. Phys. Chem. B*, 2007, **111**, 8836-8841.
17 K. K. Sharma, A. Anan, R. P. Buckley, W. Ouellette and T. Asefa, *J. Am. Chem. Soc.*, 2008, **130**, 218-228.
18 J. M. Rosenholm and M. Linden, *Chem. Mater.*, 2007, **19**, 5023-5034.
19 T. Kobayashi, D. Singappuli-Arachchige, Z. Wang, I. I. Slowing and M. Pruski, *Phys. Chem. Chem. Phys.*, 2017, **19**, 1781-1789.
20 T. Kobayashi, I. I. Slowing and M. Pruski, *J. Phys. Chem. C*, 2017, **121**, 24687-24691.
21 K. Mao, T. Kobayashi, J. W. Wiench, H.-T. Chen, C.-H. Tsai, V. S. Y. Lin and M. Pruski, *J. Am. Chem. Soc.*, 2010, **132**, 12452-12457.
22 T. Kobayashi, K. Mao, P. Paluch, A. Nowak-Krol, J. Sniechowska, Y. Nishiyama, D. T. Gryko, M. J. Potrzebowski and M. Pruski, *Angew. Chem. Int. Ed.*, 2013, **52**, 14108-14111.
23 J. R. Yates, T. N. Pham, C. J. Pickard, F. Mauri, A. M. Amado, A. M. Gil and S. P. Brown, *J. Am. Chem. Soc.*, 2005, **127**, 10216-10220.
24 M. J. Bayro, M. Huber, R. Ramachandran, T. C. Davenport, B. H. Meier, M. Ernst and R. G. Griffin, *J. Chem. Phys.*, 2009, **130**.
25 T. Kobayashi, K. Mao, S.-G. Wang, V. S. Y. Lin and M. Pruski, *Solid State Nucl. Magn. Reson.*, 2011, **39**, 65-71.
26 A. Krajnc, T. Kos, N. Z. Logar and G. Mali, *Angew. Chem. Int. Ed.*, 2015, **54**, 10535-10538.
27 I. Schnell, A. Lupulescu, S. Hafner, D. E. Demco and H. W. Spiess, *J. Magn. Reson.*, 1998, **133**, 61-69.

View Article Online
DOI: 10.1039/C8CP04425B

28 U. Friedrich, I. Schnell, D. E. Demco and H. W. Spiess, *Chem. Phys. Lett.*, 1998, **285**, 49-58.
29 L. Braunschweiler, G. Bodenhausen and R. R. Ernst, *Mol. Phys.*, 1983, **48**, 535-560.
30 D. F. Shantz, J. Gunne, H. Koller and R. F. Lobo, *J. Am. Chem. Soc.*, 2000, **122**, 6659-6663.
31 F. Blanc, C. Coperet, A. Lesage and L. Emsley, *Chem. Soc. Rev.*, 2008, **37**, 518-526.
32 K. Saalwachter, F. Lange, K. Matyjaszewski, C. F. Huang and R. Graf, *J. Magn. Reson.*, 2011, **212**, 204-215.
33 Spectral Database for Organic Compounds, SDBS., http://sdbs.db.aist.go.jp/sdbs/cgi-bin/cre_index.cgi).
34 J. Trebosc, J. W. Wiench, S. Huh, V. S. Y. Lin and M. Pruski, *J. Am. Chem. Soc.*, 2005, **127**, 3057-3068.
35 B. Grunberg, T. Emmler, E. Gedat, I. Shenderovich, G. H. Findenegg, H. H. Limbach and G. Buntkowsky, *Chem. Eur. J.*, 2004, **10**, 5689-5696.
36 K. M. Mao and M. Pruski, *J. Magn. Reson.*, 2009, **201**, 165-174.
37 A. D. Buckingham, T. Schaefer and W. G. Schneider, *J. Chem. Phys.*, 1960, **32**, 1227-1233.
38 M. J. Stephen, *Mol. Phys.*, 1958, **1**, 223-232.
39 G. Engelhardt and D. Michel, *High-resolution solid-state NMR of silicates and zeolites*, John Wiley & Sons, New York, 1987.
40 D. Singappuli-Arachchige, J. S. Manzano, L. M. Sherman and Slowing, II, *Chemphyschem*, 2016, **17**, 2982-2986.
41 M. Bak, J. T. Rasmussen and N. C. Nielsen, *J. Magn. Reson.*, 2000, **147**, 296-330.